First-principles study of stability and vibrational properties of tetragonal $PbTiO_3$

Alberto García*
Departamento de Física Aplicada II, Universidad del País Vasco, Apartado 644, 48080 Bilbao, Spain

David Vanderbilt
Department of Physics and Astronomy, Rutgers University, Piscataway, New Jersey 08855-0849
(Received 13 March 1996)

A first-principles study of the vibrational modes of $PbTiO_3$ in the ferroelectric tetragonal phase has been performed at all the main symmetry points of the Brillouin zone (BZ). The calculations use the local-density approximation and ultrasoft pseudopotentials with a plane-wave basis, and reproduce well the available experimental information on the modes at the Γ point, including the LO-TO splittings. The work was motivated in part by a previously reported transition to an orthorhombic phase at low temperatures [(J. Kobayashi, Y. Uesu, and Y. Sakemi, Phys. Rev. B **28**, 3866 (1983).] We show that a linear coupling of orthorhombic strain to one of the modes at Γ plays a role in the discussion of the possibility of this phase transition. However, no mechanical instabilities (soft modes) are found, either at Γ or at any of the other high-symmetry points of the BZ. [S0163-1829(96)04529-8]

I. INTRODUCTION

Due to their relatively simple structure and the variety of phenomena they exhibit, the perovskite oxides have become important subjects of study. Despite sharing a common formula ABO_3 and a highly symmetric high-temperature structure (Fig. 1), this family of compounds presents a rich and varied low-temperature phenomenology. Among the perovskites one finds ferroelectric crystals such as $BaTiO_3$ and $PbTiO_3$, antiferroelectrics such as $PbZrO_3$ and $NaNbO_3$, and materials such as $SrTiO_3$ that exhibit other, nonpolar instabilities.

Much progress has been made in the last 50 years in the experimental characterization of the properties of these compounds. One of the main conclusions to emerge from these studies is the fascinating dependence of the structural and dynamical behavior on details of chemical composition. Indeed, even within a given subgroup of materials one finds significantly different phase diagrams. For example, $BaTiO_3$ exhibits a complicated sequence of phase transitions, from cubic to tetragonal to orthorhombic to rhombohedral, while $PbTiO_3$ shows just one clearly established transition with $T_c = 493°C$ from the cubic paraelectric phase to a tetragonal ferroelectric structure. Moreover, the replacement of Pb for Ba also has important consequences for the dynamical processes leading to the transition. It is acknowledged that the soft mode in $BaTiO_3$ is highly overdamped, and therefore that the transition has some order-disorder flavor, whereas $PbTiO_3$ has been called a ''textbook example of displacive transition.''[1]

Until recently, however, theoretical models of perovskite properties could not properly take into account the fine chemical details that distinguish the behavior of the different materials in this family. Semi-empirical methods are not accurate enough to model the sort of delicate balance between effects (long-range dipole interactions vs short-range covalent and repulsion forces, for example), and schemes based on model Hamiltonians are usually too simple and too focused on a given material to be of much use in the unraveling of the chemical trends within the perovskites.

This situation has improved in the last few years with the use of accurate first-principles density-functional calculations to study the energy surfaces[2–4] and even the temperature-dependent phase diagrams[5–7] of various perovskite oxides. These works have achieved a high degree of success in reproducing qualitatively and even quantitatively the experimental observations, giving us confidence that one can now carry out accurate calculations to elucidate microscopic behavior (importance of hybridization, competition between long-range and short-range interactions, etc). A

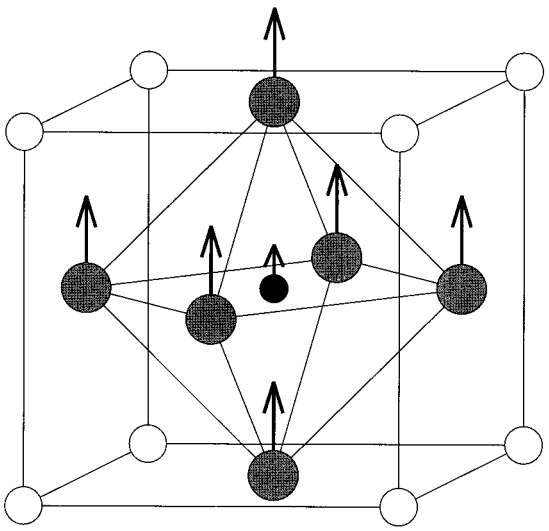

FIG. 1. Structure of ferroelectric (tetragonal) $PbTiO_3$. The arrows represent the displacements of the atoms with respect to their positions in the cubic high-temperature phase. Pb atoms are depicted by open circles, the Ti atom by the black dot in the center of the cell, and the O atoms (O_1, O_2, and O_3, displaced from the Ti atom along x, y, and z, respectively) by shaded circles.

good example is the recent work of Rabe and Waghmare,[7] which has helped revise the conventional wisdom relative to the behavior of $PbTiO_3$. Indications of a problem with the simple displacive picture were first seen experimentally in extended x-ray absorption fine-structure measurements,[8] but the theoretical work[7] has provided the microscopic underpinnings of a partial order-disorder character of the cubic-tetragonal transition in which the atomic distortions in the high-temperature phase are proposed to arise from a local instability.

Another issue, with which we will be mainly concerned in this paper, is the possible existence of a low-temperature transition. In the 1950s, Kobayashi *et al.*[9] reported the observation of what appeared to be a distorted (''multiple'') tetragonal phase of $PbTiO_3$ below approximately $-100°C$. After several negative attempts by other researchers to reproduce the observations,[10] x-ray and optical measurements were presented[11] as corroborating the existence of a low-temperature phase with an orthorhombic structure. The transition, at $-90°C$, would be second order, and bring about a very slight distortion of the tetragonal phase (with the orthorhombic cell parameters a and b differing by just 4.5×10^{-4}Å at $-194°C$) and the direction of the lattice vectors kept unchanged. The absence of superlattice reflections would imply a symmetry distortion without multiplication of the size of the unit cell.

From the point of view of the microscopic dynamics of the tetragonal structure, such a transition could be explained by a mechanical instability of a zone-center phonon whose associated atomic distortions break the tetragonal symmetry and thus relax the requirement that a and b be equal. At $T=0$ the energy surface should then present a saddle point at the configuration corresponding to the tetragonal phase, with the energy decreasing along a coordinate representing the amplitude of the soft mode and the coupled orthorhombic strain.

In this paper we have used first-principles calculations to study possible mechanical instabilities in the ferroelectric tetragonal phase of $PbTiO_3$. Our focus has been primarily on homogeneous (zone-center) distortions of the tetragonal symmetry, aimed at a detailed theoretical assessment of the possibility of the phase transition suggested by Kobayashi *et al.*[11] However, in the interest of completeness, we have also carried out an analysis of the normal modes at all the main symmetry points on the surface of the Brillouin zone (BZ). Thus we also present a fairly complete collection of normal-mode frequencies and eigenvectors for ferroelectric $PbTiO_3$ computed from first principles.

The paper is organized as follows. In Sec. II we undertake a classification of the types of possible distortions of the tetragonal phase of $PbTiO_3$ according to their symmetry. Section III briefly describes some technical aspects of our calculations, whose results are presented in Sec. IV. Section V discusses the implications of our work for the likelihood of a low-temperature transition in $PbTiO_3$. The Appendix is devoted to some issues related to the coupling of atomic displacements to strain degrees of freedom.

II. THEORETICAL ANALYSIS OF POSSIBLE INSTABILITIES

In the harmonic approximation, the calculation of phonon frequencies and mode displacement patterns involves the diagonalization of the dynamical matrix, itself obtained in a straightforward manner from the force constants $\Phi_{ij}^{\alpha\beta}$ which enter the expansion of the energy to second order in the atomic displacements,

$$E = E_0 + \sum_{ij\alpha\beta} \Phi_{ij}^{\alpha\beta} u_\alpha^i u_\beta^j . \tag{1}$$

The force constants can easily be calculated by computing all the forces caused by a given sublattice displacement.

TABLE I. Character table and decomposition of the vector and second-order symmetric tensor representations for point group $4mm$.

	E	C_4, C_4^{-1}	C_2	m_x, m_y	$m_d, m_{d'}$	V	Sym$[V\times V]$
A_1	1	1	1	1	1	z	x^2+y^2, z^2
A_2	1	1	1	-1	-1		
B_1	1	-1	1	1	-1		x^2-y^2
B_2	1	-1	1	-1	1		xy
E	2	0	-2	0	0	(x,y)	(zx,yz)

It is well-known that the normal modes of vibration of a crystal at a given k point of the BZ transform according to irreducible representations of the group of the wave vector. Thus a judicious use of the symmetry information available simplifies the analysis and saves computational work. Symmetry arguments can also profitably be used to determine the form of the series expansion of the total energy of the crystal around a given configuration, including the correct couplings among various degrees of freedom (such as atomic displacements and strains). This is precisely what is needed for a detailed study of the energy surface and the possible appearance of mechanical instabilities.

In this section we present a brief account of the use of symmetry considerations to characterize the possible instabilities of the tetragonal ferroelectric phase of $PbTiO_3$. Experimentally,[11] it has been claimed that the low-temperature structure has orthorhombic symmetry and there is no sign of cell doubling. Accordingly, we devote a subsection to the study of zone-center instabilities of orthorhombic character, and to the investigation of the form of the energy as a function of the relevant degrees of freedom. A second subsection considers distortions that might conceivably lead to a low-temperature phase transition but involve a nonorthorhombic symmetry or a doubling of the unit cell.

A. Orthorhombic instabilities with no cell doubling

The ferroelectric phase of $PbTiO_3$ (Fig. 1) is tetragonal, with space group $P4mm$. At the Γ point, the group of the wave vector is the point group of the crystal, $4mm$, characterized by a fourfold rotation axis and four symmetry planes which contain it. Table I displays the character table for $4mm$. There are five symmetry classes and thus five irreducible representations (irreps), of which one (E) is two-dimensional.

The decomposition of the vibrational representation at Γ can be shown by standard techniques to be

$$\mathrm{Vib}(\Gamma) = 4A_1 \oplus B_1 \oplus 5E . \tag{2}$$

TABLE II. Symmetry analysis of the normal modes at different points of the BZ.

k, (Group)	Irrep	No. of copies	Basis
Γ, Z $(4mm)$			
	A_1	4	$Pb_z, Ti_z, O_{1z}+O_{2z}, O_{3z}$
	B_1	1	$O_{1z}-O_{2z}$
	E	5 (2D)	$Pb_x, Ti_x, O_{1x}, O_{2x}, O_{3x}$
			$Pb_y, Ti_y, O_{1y}, O_{2y}, O_{3y}$
X, M' $(mm2)$			
	A_1	5	$Pb_z, Ti_x, O_{1z}, O_{2z}, O_{3x}$
	A_2	3	Ti_y, O_{2y}, O_{3y}
	B_1	2	Pb_y, O_{1y}
	B_2	5	$Pb_x, Ti_z, O_{1x}, O_{2z}, O_{3z}$
M, R $(4mm)$			
	A_1	2	$Pb_z, O_{1y}+O_{2x}$
	A_2	1	$O_{1x}-O_{2y}$
	B_1	1	$O_{1y}-O_{2x}$
	B_2	3	$Ti_z, O_{1x}+O_{2y}, O_{3z}$
	E	4 (2D)	$Pb_x, Ti_y, O_{2z}, O_{3y}$
			$Pb_y, Ti_x, O_{1z}, O_{3x}$

Physically, this means that the problem of diagonalizing the 15×15 dynamical matrix reduces to three simpler tasks: the diagonalization of a 4×4 matrix to decouple the four copies of the A_1 irrep, a similar 5×5 diagonalization for E, and a simple calculation of a force constant to obtain the frequency of the B_1 mode (its displacement pattern being completely determined by symmetry). The atomic motions are, therefore, coupled only within subspaces of the original 15-dimensional configuration space. The four-dimensional A_1 subspace corresponds to coupled motions with basis $[Pb_z, Ti_z, O_{1z}+O_{2z}, O_{3z}]$ and the one-dimensional B_1 subspace represents a normal mode with a displacement pattern of the form $[O_{1z}-O_{2z}]$. Of course, at Γ there are three zero-frequency acoustic modes. Two are degenerate (movements along x or y) and transform according to E, and the third is polarized along z and belongs to A_1. The complete symmetry specification of all the normal modes at Γ and at other high-symmetry k points appears in Table II.[13]

It is simple to use this symmetry information to analyze the possible mechanisms leading to the experimentally suggested phase transition from the tetragonal to an orthorhombic structure. By looking at the Γ entry in Table II and considering the characters in Table I, it can be immediately concluded that the B_1 mode has the right transformation properties. In this mode the O_1 and O_2 atoms move in opposite directions along the z axis, thus breaking the fourfold symmetry.

A calculation of the frequency of this mode is not enough to determine the existence of an instability, since one should take into account possible couplings of the atomic displacements to changes in the size and shape of the unit cell (strain variables). The possible strains that can be applied to the cell are represented by the components of a second-order symmetric tensor (η), and can be classified according to irreducible representations of the point group of the crystal as shown in the last column in Table I. In what follows we use the notation

$$r=\eta_{zz},$$

$$s=(\eta_{xx}+\eta_{yy})/2,$$

$$t=(\eta_{xx}-\eta_{yy})/2.$$

Portions of η transforming according to the identity representation A_1 leave the tetragonal symmetry unchanged. Such is the case for r and s, which refer to symmetric axial and in-plane strains, respectively. The other strain irreps are associated with lower lattice symmetries: monoclinic for E, and orthorhombic for B_1 and B_2. While a B_2 (η_{xy}) distortion leads to an orthorhombic structure with axes rotated by 45° with respect to the tetragonal basis, a pure B_1 (t) strain transforms the cell into an orthorhombic one without a change in the orientation of the axes. The latter is precisely the kind of low-temperature phase suggested for $PbTiO_3$.[11]

Apart from the change in the orientation of the axes, there is an important difference between B_2 (η_{xy}) and B_1 (t) cell distortions. Since the orthorhombic strain t transforms according to the B_1 irrep, it can couple *linearly* to the B_1 normal coordinate.[14] Therefore, the crystal energy expansion considering only the B_1 mode and strain is of the form

$$E=E_0+\tfrac{1}{2}ku^2+\tfrac{1}{2}Ct^2+\gamma ut+\cdots. \tag{3}$$

It is shown in the Appendix that the linear coupling in Eq. (3) implies a renormalization $C_{\rm eff}=C-\gamma^2/k$. Thus strain coupling could create instabilities against B_1 (orthorhombic) distortions even if the ''bare'' second-order coefficients k and C are positive.

In contrast, any coupling of the B_2 strain to a given atomic displacement u must be at least of second order,

$$E=E_0+\tfrac{1}{2}ku^2+\tfrac{1}{2}C\eta_{xy}^2++\gamma u^2\eta_{xy}^2+\alpha u^4+\beta\eta_{xy}^4+\cdots, \tag{4}$$

with no renormalization of the elastic constant C (see the Appendix).

In summary, if the purported low-temperature phase transition in $PbTiO_3$ is indeed to an orthorhombic phase with no cell doubling, and with the basis parallel to the tetragonal one, it should be linked to a negative effective elastic constant $C_{\rm eff}$ for a t strain. If one allows for the possibility of a rotation of the axes, the transition could be associated with a negative ''bare'' elastic constant for a B_2 strain.

B. Other instabilities

Apart from the experimentally suggested instability of the tetragonal phase in favor of an orthorhombic structure with no cell doubling, there are, in principle, other distortions that might conceivably lead to phase transitions. To begin with, and by reference to Table I, one could think of an instability leading to a phase with monoclinic symmetry (but still without multiplying the size of the unit cell) associated with distortions transforming according to the E irreducible representation. The analysis of this case is conceptually very similar to the one carried out for the B_1 distortions, with the difference that there are eight optical E modes capable of coupling to strain (four for each of the rows of the two-dimensional irrep E). Thus x- and y-polarized normal modes

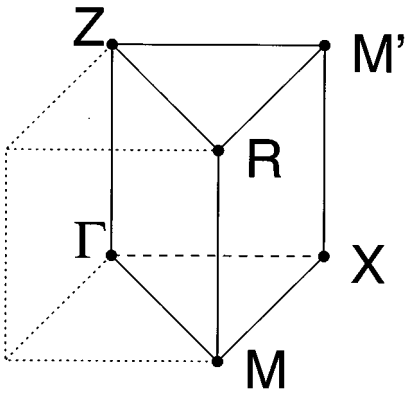

FIG. 2. Sketch showing the irreducible wedge of the Brillouin zone associated with the *P*4*mm* space group, and the positions of the symmetry points considered in this work.

will couple linearly to xz and yz strains, respectively, resulting in a renormalized elastic constant $C_{\rm eff}$ for E distortions.

Next to consider is the possibility of structural phase transitions associated with a multiplication of the size of the unit cell. These would come about through the instability of non-Γ modes. Since there is no possibility of coupling of these modes to homogeneous strain at first order, one needs only to compute the eigenvalues of the force-constant matrix to check for any saddle points in the energy surface. It is not feasible to study the modes at all the wave vectors in the BZ, so we focus on a few high-symmetry k-points on the zone surface (see Fig. 2) which represent cell-doubling distortions.

The symmetry analysis of zone-boundary modes proceeds along the same lines as those for Γ. Operations that leave the wave vector invariant will, in general, form subgroups of $4mm$. For the purposes of our work it suffices to consider just one more point group, $mm2$, whose character table is given in Table III.[12] We show the symmetry decomposition of atomic displacements at the zone-boundary points in Table II.

III. DETAILS OF CALCULATIONS

The determination of the force constants involves the consideration of appropriately distorted crystal configurations. Symmetry arguments are used to reduce to the minimum the number of different calculations that need to be carried out, and to obtain the relevant information in the most direct form. For z-polarized modes at the Γ point, for example, it is only necessary to consider the four linearly independent atomic distortions (1,0,0,0,0), (0,1,0,0,0), $(0,0,1,-1,0)/\sqrt{2}$, and $(0,0,1,1,-2)/\sqrt{6}$, where the basis is formed by unit z displacements of Pb, Ti, O_1, O_2, and O_3.

TABLE III. Character table for the point group $mm2$. The symbols m_1,m_2 stand for m_x, m_y or m_d, $m_{d'}$, depending on the orientation of the axes.

	E	C_2	m_1	m_y
A_1	1	1	1	1
A_2	1	1	-1	-1
B_1	1	-1	1	-1
B_2	1	-1	-1	1

Strain parameters are determined by subjecting the crystal to pure strains and fitting the energy to a polynomial form. The strain-phonon couplings are computed by finding the forces on the atoms caused by a suitable strain, since, from Eq. (3),

$$\left(\frac{\partial E}{\partial u}\right)_{u=0} = \gamma t. \tag{5}$$

We use ultrasoft pseudopotentials, a plane-wave basis set, and a conjugate-gradients algorithm to compute total energies and forces for a variety of crystal configurations. The method and the details of the pseudopotentials employed have been described elsewhere.[4] For this work we find that a (4,4,4) Monkhorst-Pack[15] sampling of the BZ is enough to provide good precision in the calculated coefficients (see next section). Force constants are computed using the Hellmann-Feynman theorem, with atomic displacements of 0.002 in lattice units.

A final methodological note concerns the calculation of the frequencies of longitudinal optic (LO) modes at the Γ point. Since our calculations use periodic boundary conditions, we are not able to introduce a macroscopic electric field, such as it would arise in an ionic crystal in the presence of a $q\rightarrow 0$ longitudinal vibration. This field creates a splitting of the frequencies of infrared-active phonons, with the coupling constants being the ionic effective charges Z^*. The force-constant matrix has to be augmented by the effect of a screened (by electronic effects only) Coulomb interaction among those effective charges,

$$\Phi_{ij}^{\alpha\beta}\rightarrow\Phi_{ij}^{\alpha\beta}+\frac{4\pi e^2}{\Omega\epsilon_\infty}Z_i^*Z_j^*. \tag{6}$$

The effective charges can be obtained from first-principles calculations. Here we use those computed for cubic $PbTiO_3$ by Zhong and Vanderbilt.[16]

IV. RESULTS

A first concern is the determination of the structural parameters of the ferroelectric tetragonal phase of $PbTiO_3$. First-principles LDA calculations typically underestimate the lattice constants of perovskite oxides by around 1%. Our final objective is the study of dynamical properties of the crystal, and it would be debatable whether it is better to compute phonon frequencies and other dynamical parameters at the experimental or at the theoretical lattice constant. Past experience with perovskites has shown that the displacement patterns associated with some soft modes, and even the existence of the latter, depend on lattice constant and strain.[2,3] In the case of ferroelectric $PbTiO_3$ there is an additional complication, namely the existence of internal atomic displacements, which are of course coupled to the cell dimensions. Our first strategy was to use the experimental lattice constants $a=7.380$ a.u., $c/a=1.0635$ and optimize the internal atomic positions to obtain a base reference configuration with zero forces with which to compute phonon frequencies and strain coefficients. We call this ''Theory I.'' Later we determined an optimized structure (cell shape and atomic positions coupled) via a special minimization proce-

TABLE IV. Structural parameters of $PbTiO_3$. Theory I and II refer to a relaxation with constrained lattice constants, and a free relaxation, respectively. z atomic coordinates are given in lattice units. Experimental values are taken from Ref. 21.

	Theory I	Theory II	Experiment
a (a.u.)	7.380	7.298	7.380
c/a	1.063	1.054	1.063
z(Ti)	0.549	0.537	0.540
$z(O_1,O_2)$	0.630	0.611	0.612
$z(O_3)$	0.125	0.100	0.112

dure (see the Appendix); we call this ''Theory II.'' Table IV summarizes the structural information. While, as we shall see, we obtain substantially the same phonon frequencies in either case, the second approach, using as a reference the structure which gives a theoretical energy minimum with respect to strain, is, in principle, more appropriate for the calculation of elastic properties and strain-phonon couplings.

As part of the investigation of the possible mechanical instabilities,[17] we have obtained a complete set of calculated phonon frequencies for $PbTiO_3$. These are given, along with experimental results when available, in Tables V and VI.[18] The agreement of our theoretical results with experiment for the zone-center modes (both TO and LO) is quite good. We are thus confident that our computational approach can be trusted in its predictions of zone-edge vibrational frequencies that have not yet been determined experimentally. To our knowledge, the only other calculation of vibrational frequencies and modes for tetragonal $PbTiO_3$ was carried out by Freire and Katiyar.[19] An important difference with our work is that those authors used an empirical fitting procedure to adjust the parameters of a rigid-ion model. We use no empirical parameters of any kind, just the atomic numbers and masses of the atoms involved. Table V can be used also to estimate the degree of dependence of the phonon frequencies upon the details of the base structure used in the calculations (''Theory I'' or ''Theory II'' above). Phonons at zone-boundary points are computed using the ''Theory I'' structure.

TABLE V. Frequencies of optical modes at Γ in cm^{-1}. Infrared-active modes exhibit LO-TO splitting. See text and Table IV for the meaning of Theory I and Theory II. Experimental values as compiled in Ref. 19.

	Theory I	Theory II	Experiment
A_1(TO)	151	146	147
A_1(TO)	355	337	359
A_1(TO)	645	623	646
E(TO)	81	82	88
E(TO)	183	195	220
E(TO)	268	237	289
E(TO)	464	501	505
B_1	285	280	289
A_1(LO)	187	186	189
A_1(LO)	449	447	465
A_1(LO)	826	799	796
E(LO)	114	125	128
E(LO)	267	273	289
E(LO)	435	418	436
E(LO)	625	675	723

TABLE VI. Computed frequencies of zone-edge phonons, classified by symmetry label. The base structure used in the calculations is Theory I of Table IV. Experimental values are given when available (Ref. 19).

k	Irrep	Frequencies (cm^{-1})	Expt.
Z	A_1	102, 189, 447, 831	
	B_1	292	
	E (2)	46, 151, 184, 270, 454	59, 168
X	A_1	66, 237, 285, 309, 486	72
	A_2	131, 233, 426	
	B_1	54, 321	
	B_2	99, 177, 337, 608, 672	
M	A_1	74, 452	
	A_2	412	
	B_1	138	
	B_2	247, 635, 716	
	E (2)	57, 203, 294, 398	
M'	A_1	67, 110, 272, 406, 415	
	A_2	152, 270, 401	
	B_1	57, 329	
	B_2	58, 188, 312, 579, 794	
R	A_1	90, 411	
	A_2	401	
	B_1	135	
	B_2	200, 626, 803	
	E (2)	65, 136, 322, 386	

To test the convergence of our results with respect to the density of the k-point grid for BZ integrations, we recomputed the frequencies of z-polarized Γ modes using a (6,6,6) Monkhorst-Pack grid. The results, displayed in Table VII, indicate a high level of convergence.

As for the question of the existence of a phase transition at low temperature, we find that all the vibrational frequencies are real, as can be seen from the positive sign of all the mode force constants k. Thus there are no mechanical instabilities in the ''bare'' vibrational degrees of freedom, either at Γ or at the edges of the BZ. However, there still remains

TABLE VII. Test of the convergence of mode frequencies with k-point grid. (4,4,4) and (6,6,6) grids are used for the ''Theory I'' choice of Table IV. The frequencies (in cm^{-1}) are those of the transverse z-polarized modes at Γ.

k-point grid	(4,4,4)	(6,6,6)
A_1(TO)	151	153
B_1	285	289
A_1(TO)	355	359
A_1(TO)	645	648

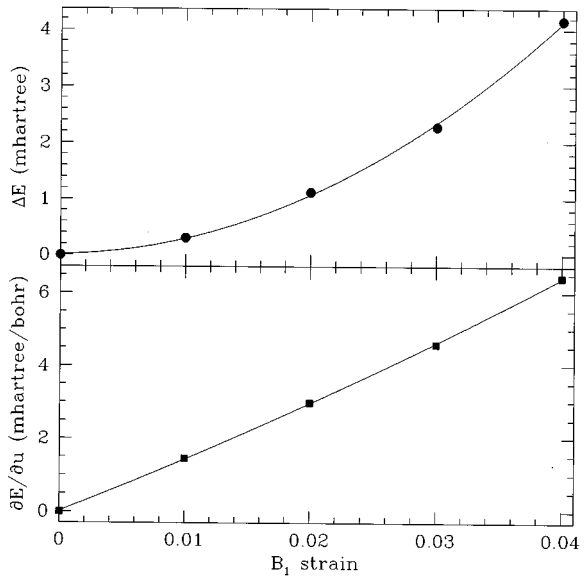

FIG. 3. Upper panel: Change in crystal energy (per cell) as a function of the orthorhombicity parameter t (B_1 strain). The curve is a fit to a parabola. Lower panel: Derivative of the crystal energy with respect to the B_1 normal mode amplitude at zero amplitude, as a function of B_1 strain. According to Eq. (5), it measures the degree of coupling between the normal mode and the strain.

the question of whether the linear coupling to strain degrees of freedom could result in any instability.

We deal first with the renormalization of the elastic constant corresponding to a B_1 orthorhombic strain. By applying pure B_1 strains of different magnitudes (for which we set $b-a\neq 0$ while keeping the sum $a+b$ constant) and computing the resulting values of the total energy, we obtain the data plotted in Fig. 3. A fit to a simple parabola is very good up to sizable strains. The elastic constant C [see Eq. (3)] turns out to be 5.0 hartree.[20] As mentioned above, we use the optimized structure (''Theory II'') for this and the rest of the calculations involving elastic constants and strain-phonon couplings.

From the same set of calculations, but extracting this time the forces on the atoms and taking the scalar product (in configuration space) with the eigenvector of the B_1 mode, we obtain from Eq. (5) (see also Fig. 3) $\gamma=0.15$ hartree/bohr. The force constant for the B_1 mode is 0.048 hartree/bohr^2, so the renormalized C is $C_{\rm eff}=4.5$ hartree. We see that even though there is a 10% change in the value of the elastic constant, the renormalization due to the coupling to the phonons is not enough to cause a B_1 instability of the tetragonal cell.

We performed a similar set of calculations for the analysis of the monoclinic distortion with E symmetry. The forces along the x axis appearing upon application of an η_{xz} strain translated into coupling constants of 0.17, 0.05, 0.06, and 0.00 hartree for the optical x-polarized E modes of respective force constants 0.014, 0.042, 0.077, and 0.155 hartree/bohr^2. The bare elastic constant for η_{xz} strain is 5.4 hartree. Adding up the contributions to the renormalization from the four modes we obtained an effective elastic constant $C_{\rm eff}$ of 3.3 hartree. In this case the renormalization amounts to 40% of the bare value, but still is not enough to drive an E instability.

As discussed above, there is no linear coupling of B_2 orthorhombic strains to atomic displacements. The calculated elastic constant for this type of strain is positive (6.0 hartree), so there should be no instabilities of B_2 symmetry either.

Finally, recall that there is no first-order coupling of zone-boundary modes to homogeneous strain. Thus we need only check the bare force constants, which are all found to be positive (see Table VI). This means that we do not expect any mechanical instabilities associated with a cell doubling.

V. CONCLUSIONS

The low-temperature transition proposed by Kobayashi *et al.*[11] on the basis of x-ray and optical measurements is supposed to involve a slight orthorhombic distortion of the tetragonal phase, maintaining the orientation of the cell axes with no cell doubling. Our analysis of the energetics of B_1 distortions shows that a low-temperature transition of this kind is possible, in principle, but not likely in ferroelectric $PbTiO_3$. In this connection, it should be noted that, to our knowledge, the experimental observations of Ref. 11 have not been reproduced since 1983.

We also checked more generally for other kinds of low-temperature structural transitions. However, we find that all unit-cell-preserving distortions exhibit positive elastic constants, thus apparently ruling out transitions to a monoclinic structure (E distortions) or to a 45°-rotated orthorhombic structure (B_2 strain). Furthermore, we show that there are no mechanical instabilities associated with zone-boundary normal modes that could cause a phase transition with cell doubling.

Since we have not exhaustively explored the vibrational spectrum of the crystal, it is conceivable that a mechanical instability at a k point not on the BZ boundary may have been missed. However, our work shows fairly clearly that a simple transition is not likely in ferroelectric $PbTiO_3$ at low temperatures.

Note added in proof. After this paper had been submitted for publication, we learned of a set of high-resolution x-ray and neutron diffraction experiments on powder $PbTiO_3$ samples which appear to indicate that $PbTiO_3$ remains tetragonal down to 10 K [J. M. Kiat (private communication)].

ACKNOWLEDGMENTS

This work was supported in part by the ONR Grant N00014-91-J-1184 and by the UPV research Grant No. 060.310-EA149/95. Thanks are due to J.M. Pérez-Mato, M. Aroyo, W. Zhong, and U. Waghmare for useful comments.

APPENDIX

1. Renormalization of energy-surface coefficients

We show first how the linear coupling of u to t in the energy expansion of Eq. (3) implies a renormalization of C (or, equivalently, of k). After a transformation of the quadratic form to ''principal axes'' by a linear change of vari-

ables, the first partial derivatives of the energy will be zero. We can achieve the transformation implicitly by setting the derivative of E with respect to u to zero, and solving for u, to get $u=-\gamma t/k$. When this condition is inserted back into Eq. (3), we obtain an expression for E as a function of the free variable t,

$$E(t)=\frac{1}{2}\left(C-\frac{\gamma^2}{k}\right)t^2=\frac{1}{2}C_{\text{eff}}t^2, \tag{A1}$$

from which it follows that the effective elastic constant is $C_{\text{eff}}=C-\gamma^2/k$. (If instead u is chosen as a free variable, one obtains a renormalized spring constant $k_{\text{eff}}=k-\gamma^2/C$. However, the physical mode frequency is not renormalized, because of the ''infinite mass'' associated with the strain degrees of freedom.)

In the case of the B_2 distortion with quadratic coupling, Eq. (4), one needs $\beta>0$ and $\alpha>0$ or else there would be unphysical divergences to $-\infty$ in the energy. But then, setting the u derivative of the energy to zero, one gets either $u=0$ (trivial) or $u^2=-(k+2\gamma t^2)/4\alpha$ (meaningless since u would be imaginary). Thus there is no renormalization of the elastic constant.

2. Optimization of structural parameters

Using the symmetry constraints of the $4mm$ point group, one can write down the expression (to second order in the strain and atomic displacements) for the energy of a general tetragonal phase of that symmetry as

$$E=E_0+E_{\text{strain}}+E_{\text{internal}}+E_{\text{strain-ph}}, \tag{A2}$$

where

$$E_{\text{strain}}=\alpha_1 s+\beta_1 r+\alpha_2 s^2+\beta_2 r^2+\delta s r \tag{A3}$$

is the part that depends only on the s and r strains,

$$E_{\text{internal}}=\sum_{i=1}^{3}\tfrac{1}{2}k_i u_i^2 \tag{A4}$$

is the change in energy due to internal atomic displacements compatible with the symmetry (and thus expanded as combinations of the three A_1 phonons polarized along the z axis), and

$$E_{\text{strain-ph}}=\sum_{i=1}^{3}(\gamma_s^i u_i s+\gamma_r^i u_i r) \tag{A5}$$

are the symmetry-allowed couplings of s and r to the A_1 phonons (both s and r transform according to A_1).

The 14 coefficients in this expansion are easily computed for a given base configuration. In our case, the starting point is a tetragonal cell with a and c given by experiment and the internal atomic positions along the z axis optimized theoretically to eliminate residual forces (column labeled ''Theory I'' in Table IV). Computed A_1 phonon frequencies directly give the force constants k_i, and the strain and strain-coupling coefficients are obtained in a manner analogous to that described in the main body of the paper. Once the quadratic form for E is known, it is a simple matter to find the structural parameters which correspond to the minimum energy (column labeled ''Theory II'' in Table IV). As is typical of first-principles calculations, the calculated lattice parameters are smaller than the experimental values by around 1%.

*Electronic address: wdpgaara@lg.ehu.es; FAX: +34-4-464-8500.

[1] For a good discussion of the experimental work on perovskites, see M.E. Lines and A.M. Glass, *Principles and Applications of Ferroelectric and Related Materials* (Clarendon, Oxford, 1977).

[2] R.E. Cohen and H. Krakauer, Phys. Rev. B **42**, 6416 (1990); Ferroelectrics **136**, 65 (1992); R.E. Cohen, Nature (London) **358**, 136 (1992).

[3] D.J. Singh and L.L. Boyer, Ferroelectrics **136**, 95 (1992).

[4] R.D. King-Smith and D. Vanderbilt, Phys. Rev. B **49**, 5828 (1994); Ferroelectrics **136**, 85 (1992).

[5] W. Zhong, D. Vanderbilt, and K.M. Rabe, Phys. Rev. Lett. **73**, 1861 (1994); Phys. Rev. B **52**, 6301 (1995).

[6] W. Zhong and D. Vanderbilt, Phys. Rev. Lett. **74**, 2587 (1995).

[7] K.M. Rabe and U.V. Waghmare, J. Phys. Chem. Solids (to be published).

[8] N. Sicron, B. Ravel, Y. Yacoby, E.A. Stern, F. Dogan, and J.J. Rehr, Phys. Rev. B **50**, 13 168 (1994).

[9] J. Kobayashi and R. Ueda, Phys. Rev. **99**, 1900 (1955); J. Kobayashi, S. Okamoto, and R. Ueda, Phys. Rev. **103**, 830 (1956).

[10] See, for example, S.A. Mabud and A.M. Glazer, J. Appl. Crystallogr. **12**, 49 (1979).

[11] J. Kobayashi, Y. Uesu, and Y. Sakemi, Phys. Rev. B **28**, 3866 (1983).

[12] Since the notation for irreducible representations at different points of the BZ is not standardized, we prefer to use the customary irrep labeling for point groups (A, B, E, etc.) and refer to specific representations by mentioning the k point explicitly.

[13] Note that some k points have the same irrep classification. In fact, whole lines of the BZ belong to the same ''symmetry class.'' The term *Wintgen position* has been coined for such symmetry-equivalent points in reciprocal space, in analogy with the standard *Wyckoff positions* of the real-space description. See M.I. Aroyo and H. Wondratschek, Z. Kristallogr. **210**, 243 (1995).

[14] The crystal energy, being invariant against all the symmetry operations, must transform according to the identity (A_1) representation. It is a well-known result of group theory that the identity can always be obtained by the product of a given irrep with itself. For a discussion of the influence of these couplings in the elastic and piezoelectric response of a crystal, see P.B. Miller and J.D. Axe, Phys. Rev. **163**, 924 (1967).

[15] H.J. Monkhorst and J.D. Pack, Phys. Rev. B **13**, 5188 (1976).

[16] See for example, W. Zhong and D. Vanderbilt, Phys. Rev. Lett. **72**, 3618 (1994).

[17] For the purpose of discussing mechanical instabilities, one does not need to take into account the masses of the atoms; it suffices to analyze the eigenvectors and eigenvalues of the force-constant matrix. However, once this matrix is determined, it is straightforward to include the relevant mass factors to obtain the dynamical matrix and phonon frequencies (and to augment the dynamical matrix with the long-range Coulomb coupling terms to get the LO-TO splitting).

[18] The mode eigenvectors are not listed, but can be obtained from the authors upon request.
[19] J. D. Freire and R. S. Katiyar, Phys. Rev. B **37**, 2074 (1988).
[20] Our energies in Eqs. (3) and (4) are referred to a fixed cell volume. It is customary to give elastic constants in units of energy/volume; we are implicitly using units of energy/cell.
[21] F. Jona and G. Shirane, *Ferroelectric Crystals* (Dover, New York, 1993).